

AperTO - Archivio Istituzionale Open Access dell'Università di Torino

Parallel dual secondary column-dual detection: A further way of enhancing the informative potential of two-dimensional comprehensive gas chromatography

This is the author's manuscript

Original Citation:

Availability:

This version is available <http://hdl.handle.net/2318/148168> since 2016-12-01T13:10:54Z

Published version:

DOI:10.1016/j.chroma.2014.07.081

Terms of use:

Open Access

Anyone can freely access the full text of works made available as "Open Access". Works made available under a Creative Commons license can be used according to the terms and conditions of said license. Use of all other works requires consent of the right holder (author or publisher) if not exempted from copyright protection by the applicable law.

(Article begins on next page)



UNIVERSITÀ DEGLI STUDI DI TORINO

This Accepted Author Manuscript (AAM) is copyrighted and published by Elsevier. It is posted here by agreement between Elsevier and the University of Turin. Changes resulting from the publishing process - such as editing, corrections, structural formatting, and other quality control mechanisms - may not be reflected in this version of the text. The definitive version of the text was subsequently published in [*Journal of Chromatography A*, Volume 1360, 19 September 2014, Pages 264–274. DOI: 10.1016/j.chroma.2014.07.081].

You may download, copy and otherwise use the AAM for non-commercial purposes provided that your license is limited by the following restrictions:

- (1) You may use this AAM for non-commercial purposes only under the terms of the CC-BY-NC-ND license.
- (2) The integrity of the work and identification of the author, copyright owner, and publisher must be preserved in any copy.
- (3) You must attribute this AAM in the following format: Creative Commons BY-NC-ND license (<http://creativecommons.org/licenses/by-nc-nd/4.0/deed.en>), [<http://dx.doi.org/10.1016/j.chroma.2014.07.081>]

1 **Parallel dual secondary column-dual detection:**
2 **a further way of enhancing the informative potential of two-dimensional**
3 **comprehensive gas chromatography**

4
5 Luca Nicolotti¹, Chiara Cordero^{2*}, Davide Bressanello², Cecilia Cagliero², Erica Liberto², Federico Magagna²,
6 Patrizia Rubiolo², Barbara Sgorbini² and Carlo Bicchi²

7
8
9
10 ¹Author's affiliation:

11 Faculty of Chemistry, Technical University of Munich; Lise-Meitner-Strasse 34, 85354 Freising, Germany

12
13 ²Authors' affiliation:

14 Dipartimento di Scienza e Tecnologia del Farmaco, Università di Torino, Via Pietro Giuria 9, I-10125 Turin,
15 Italy

16
17 * Address for correspondence:

18 Dr. Chiara Cordero - Dipartimento di Scienza e Tecnologia del Farmaco, Università di Torino, Via Pietro
19 Giuria 9, I-10125 Torino, Italy – e-mail: chiara.cordero@unito.it ; phone: +39 011 6707662; fax: +39 011
20 2367662

21
22
23

24 **Abstract**

25 Comprehensive two-dimensional gas chromatography (GC×GC) coupled with Mass Spectrometry (MS) is
26 one of today's most powerful analytical platforms for detailed analysis of medium-to-high complexity
27 samples. The column set usually consists of a long, conventional-inner-diameter first dimension (¹D)
28 (typically 15-30 m long, 0.32-0.25 mm d_c), and a short, narrow-bore second dimension (²D) column
29 (typically 0.5-2 m, 0.1 mm d_c) where separation is run in a few seconds. However, when thermal
30 modulation is used, since the columns of a set are coupled in series, a flow mismatch occurs between the
31 two dimensions, making it impossible to operate simultaneously at optimized flow conditions. Further,
32 short narrow-bore capillaries can easily be overloaded, because of their lower loadability, limiting the
33 effectiveness of ²D separation.

34 In this study, improved gas linear velocities in both chromatographic dimensions were achieved by coupling
35 the ¹D column with two parallel ²D columns, having identical inner diameter, stationary phase chemistry,
36 and film thickness. In turn, these were connected to two detectors: a fast quadrupole Mass Spectrometer
37 (MS) and a Flame Ionization Detector (FID). Different configurations were tested and performances
38 compared to a conventional set-up; experimental results on two model mixtures (*n*-alkanes and fourteen
39 medium-to-high polarity volatiles of interest in the flavor and fragrance field) and on the essential oil of
40 *Artemisia umbelliformis* Lam., show the system provides consistent results, in terms of analyte
41 identification (reliability of spectra and MS matching) and quantitation, also affording an internal cross-
42 validation of quantitation accuracy.

43

44

45 **Key-words:**

46 Two-dimensional comprehensive gas chromatography-mass spectrometry; parallel dual secondary column-
47 dual detection; dual ²D pattern alignment, outlet pressure correction, second dimension linear velocity
48 optimization, essential oil analysis

49

50 1. Introduction

51 Comprehensive two-dimensional gas chromatography (GC×GC) coupled with Mass Spectrometry
52 (MS) is one of the most powerful analytical platforms now available for the detailed analysis (identification
53 and quantitation) of medium-to-high complexity samples. Compared to one-dimensional systems, it offers
54 remarkable separation power and unmatched peak capacity [1,2]; the possibility of applying different
55 separation mechanisms in the two chromatographic dimensions produces rationalized 2D patterns, suitable
56 as sample fingerprints for classification and identification purposes [3].

57 The most common GC×GC column sets consist of a long, conventional-inner-diameter first dimension (¹D)
58 (typically 15-30 m long and 0.32-0.25 mm d_c), and a short, narrow-bore second dimension (²D) column
59 (typically 0.5–2 m 0.1 mm d_c). Thanks to the short narrow-bore ²D column, the separation is run in a few
60 seconds, both minimizing wrap-around phenomena and contributing to the high efficiency of the system.
61 However, when thermal modulation is used, since the columns of a set are coupled in series, a flow
62 mismatch occurs between the two dimensions; this makes it impossible to operate simultaneously at
63 optimized flow conditions. In addition, short narrow-bore capillaries can easily overload, because of their
64 lower loadability, limiting ²D separation effectiveness [4,5]. The configuration and optimization of a GC×GC
65 set-up is thus a crucial, but also a complex step, since separation in the two dimensions is differently
66 influenced in the two separation dimensions by carrier gas flow, temperature, and modulation period. With
67 regard to the flow regime, in their earlier publications Phillips *et al* [6,7] indicated a possible way of
68 optimizing carrier gas flow by splitting part of the flow from ¹D to waste, prior to modulation. They adopted
69 a Tee union to connect the two analytical columns, and a short capillary segment enabling the diversion of
70 about 30% of the primary column flow to waste, thus applying flows closer to the optimal in both
71 dimensions, and reducing overloading of the ²D.

72 In 2007, Tranchida *et al.* [8] included a flow splitter in a classical GC×GC-FID system. The method, called
73 “split-flow” comprehensive 2D-GC, consisted of a ¹D apolar 30 m × 0.25 mm d_c column, connected to a 1 m
74 × 0.10 mm d_c polar ²D and to an uncoated capillary of 30 cm × 0.10 mm d_c , using a Y press fit. The carrier
75 gas (hydrogen) linear velocities were regulated thanks to a manually-operated split valve, connected to the
76 uncoated capillary. Experimental results on Fatty Acids Methyl Esters (FAMES) from a cod oil sample
77 showed that, with a 35:65 (FID) split-flow ratio and 146.3 kPa head pressure, gas velocities close to optimal
78 could be obtained (i.e., about 35 and 213 cm/sec in the ¹D and ²D respectively) with a positive effect on
79 separation efficiency and resolution (+50% for a selected critical pair) while maintaining structured
80 chromatograms.

81 Other straightforward solutions have been proposed to overcome this critical issue, which is known as flow-
82 mismatch in the two dimensions. In stop-flow GC×GC [9-11] the ¹D flow is periodically halted and during
83 each pause the ²D separation continues, by delivering carrier gas via an auxiliary pressure controller. This

84 latter set-up enables column flow to be independently regulated, thus optimizing the separation in both
85 dimensions.

86 Another possibility is to adopt wider ²D capillaries [12,13]; if columns of a set have the same inner
87 diameter, flow conditions closer to optimal can be applied in both dimensions, improving the exploitation
88 of the ²D stationary phase selectivity, even at higher temperature rates, and at the same time increasing ²D
89 column loadability [12]. Experimental results on medium-complexity samples of interest in the flavor and
90 fragrance field, with homologous d_c column sets, show that the mean loss of peak capacity (by a factor of 3;
91 System Separation Measure - $S_{GC \times GC}$) is partially or fully compensated, thanks to better exploitation of ²D
92 stationary phase selectivity. At the same time, reliable quali-quantitative results are achieved, by complying
93 with the minimal modulation requirements (Modulation Ratio criterion - M_R) [13]. More recently, Peroni *et*
94 *al.* evaluated two alternative solutions: (a) the use of monolithic ²D columns [14], and (b) multiple capillary
95 columns in parallel as ²D [15]. With monoliths, efficiency and column flow can be optimized independently,
96 but at the cost of poor separation efficiency. However, multi-²D columns appear to be a good alternative;
97 the carrier gas flow is divided over multiple-parallel ²D flow paths, enabling both dimensions to be fully
98 exploited at the same time. Unfortunately, as the authors themselves state, coupling the ¹D to the multi-²D
99 is, in practice, rather a complex procedure, limiting the feasibility of such set-ups in routine use.

100 As discussed by Peroni and Janssen [16], the optimum linear velocities in both dimensions are reduced
101 when the second dimension operates at high outlet pressure. The proposed set-up includes a restrictor at
102 the outlet of the ²D, prepared by melting the end of the column with a high-temperature hydrogen flame
103 (1800°C) until closure, and then partially re-opening it, by grinding it with sandpaper, to obtain the desired
104 flow. The elevated outlet pressure conditions resulted in flatter *Van Deemter* curves at higher velocities,
105 causing a slower loss of efficiency at higher inlet pressures. Experimental results indicated that this system
106 configuration is characterized by a slightly improved resolution for a given column set, compared to
107 conventional pressure drops, but that the analysis time is longer.

108 In the present study, improved gas linear velocities in both chromatographic dimensions were achieved by
109 coupling the ¹D column with two parallel ²D columns having identical inner diameter, stationary phase
110 chemistry, and film thickness, in turn connected to two detectors: a fast quadrupole Mass Spectrometer
111 (MS), and a Flame Ionization Detector (FID). The system was equipped with a loop-type thermal modulator;
112 cryotrapping and refocusing were set at the head of the ²D capillaries to narrow bands entering the ²D
113 [17]. Three different column set-up were tested: the first, *Set-up I*, included a primary column connected
114 with two parallel ²Ds of different lengths (1.6 m x 0.1 mm d_c to MS and 1.4 m x 0.1 mm d_c to FID) but
115 operating at an almost equal nominal flow (comparable hold-up times) although subjected to different
116 outlet pressures. The second system configuration, *Set-up II*, included two identical ²D columns (1.4 m x 0.1
117 mm d_c) and an auxiliary pressure controller to deliver a supplementary flow of carrier gas at the outlet of
118 the ²D connected to the MS detector. The latter was inspired by the system proposed by Shellie *et al.* [18],

119 in which GC×GC-FID and GC×GC-TOF-MS chromatograms were successfully matched, obtaining almost
120 identical 2D patterns thanks to the adjustment of inner and outlet pressures. Lastly a conventional set-up
121 was taken as a reference, i.e. *Set-up III* consisted of a single ²D column (total length including modulation
122 loop: 1.4 m x 0.1 mm *d_c*) connected to two parallel detectors, via splitting capillaries.

123 The performance of each *Set-up* are evaluated by analyzing two model mixtures (n-alkanes (HydStd1) and
124 14 medium-to-high polarity volatiles in the flavor and fragrance field (FFStd2)), and the *Artemisia*
125 *umbelliformis* Lam. essential oil. The potentials and limits of each set-up are also discussed in terms of
126 separation performances and in view of the practical information that can be derived from each single
127 analytical run.

128

129 **2. Experimental**

130 **2.1 Samples and solvents**

131 Pure standards of *n*-alkanes (from *n*-C9 to *n*-C25) for system evaluation, flow/pressure optimization and
132 Linear Retention Indices (*I_T*) determination were from Sigma-Aldrich (Milan, Italy).

133 Pure standards of α-pinene, benzaldehyde, benzyl alcohol, α-thujone, camphor, carvone, cinnamyl alcohol,
134 geranyl acetate, vanillin, coumarin, isoeugenol, isoeugenyl acetate, benzyl benzoate, and sclareol, were
135 from Sigma-Aldrich (Milan, Italy). The two model mixtures (i.e., HydStd1 and FFStd2) for system evaluation
136 were prepared by mixing single component Standard Mother Solutions, at 10 g/L in dichloromethane, and
137 adjusting the final volume up to 100 mg/L. Solvents were all HPLC-grade, from Riedel-de Haen (Seelze,
138 Germany).

139 *Artemisia umbelliformis* Lam. essential oil (EO) was prepared following the method of the European
140 Pharmacopoeia [19]. Ten grams of dried aerial parts from experimental cultivations run in different alpine
141 valleys were suspended in 250 mL of water in a 500 mL flask for 1 h, and then submitted to hydrodistillation
142 in a Clevenger micro-apparatus for 2 hours [20]. The resulting EO was left to stabilize for 1 h, then
143 recovered and analyzed directly.

144

145 **2.2 GC×GC instrument set-up**

146 GC×GC analyses were run with a system configured as follows: a HT280T multipurpose sampler (HTA,
147 Brescia, Italy) was integrated with an Agilent 6890 GC unit coupled to an Agilent 5975C MS detector
148 (Agilent, Little Falls, DE, USA) operating in EI mode at 70 eV. The GC transfer line was set at 280°C. A
149 *Standard Tune* was used and the scan range was set to *m/z* 40-300 with a scanning rate of 12,500 amu/s to
150 obtain a spectra generation frequency of 28 Hz. The Flame Ionization Detector (FID) conditions were: base
151 temperature 280°C, H₂ flow 40 mL/min; air flow 240 mL/min; make-up (N₂) 450 mL/min; sampling
152 frequency 150 Hz.

153 Injections of the essential oil, and of the two model mixtures, as well as those for I_s^T determination
154 samples, were by HT280T sampler (HTA, Brescia, Italy) under the following conditions: split/splitless
155 injector, split mode, split ratio 1/50, injector temperature 280°C, injection volume 0.1 μ L of undiluted
156 essential oil and 1 μ L of the *n*-HydStd1 and FFSTd2 model mixtures at 100 mg/L. The oven temperature was
157 programmed as follows: 50°C (1 min) to 270°C at 3.0°C/min and to 290°C at 10°C/min (10 min).

158 Flow/pressure optimization was checked on a standard solution of tridecane, tetradecane and pentadecane
159 (n-C13 to n-C15) at 100 mg/L analyzed in isothermal conditions at 150°C. Head-pressure values are
160 reported in **Table 1**.

161

162 **2.3 Thermal modulator parameters**

163 The system was equipped with a two-stage KT 2004 loop thermal modulator (Zoex Corporation, Houston,
164 TX) cooled with liquid nitrogen controlled by Optimode™ V.2 (SRA Instruments, Cernusco sul Naviglio, MI,
165 Italy). Hot jet pulse time was set at 250 ms, modulation time was 5 s and cold-jet total flow progressively
166 reduced with a linear function, from 40% of Mass Flow Controller (MFC) at initial conditions, to 5% at the
167 end of the run. Loop dimensions were chosen on the basis of the expected carrier linear velocities, to
168 ascertain that at least two stage-band-focusing releases were performed for each modulation. Thus, for all
169 *Set-ups*, the first 0.6 m of the 2 Ds was wrapped in the metal slit of the modulator.

170

171 **2.4 Column connections and auxiliary control module**

172 Connections between the primary and the two secondary columns (*Set-ups I and II*), and between the
173 secondary column and the deactivated capillaries for FID/MS effluent splitting (*Set-up III*) was via a SilFlow™
174 GC 3 Port Splitter (SGE Ringwood, Victoria, Australia). The auxiliary pressure controller consisted of a one
175 channel Pneumatics Control Module (G2317A) connected to a Quick Swap unit (G3185, Agilent, Little Falls,
176 DE, USA) with a restrictor capillary of 0.17 m x 0.1 mm d_c . A diagram of the system configuration is provided
177 as Supplementary File (Supplementary Figure 1 - SF1).

178 Column set configurations are listed in **Table 1**, together with carrier gas head pressures and calculated
179 linear velocities [18,21].

180

181 **2.5 Data acquisition and 2D plot elaboration**

182 Data were acquired by Agilent MSD ChemStation ver D.02.00.275 and processed using GC Image GC×GC
183 Software version 2.1b1 (GC Image, LLC Lincoln NE, USA).

184

185 **3. Results and discussion**

186 **3.1 Some theoretical aspects**

187 Conventional GC×GC configurations with thermal modulators imply that the two columns of the set are
188 connected in series and the volumetric flow rates and linear velocities in the two capillaries are correctly
189 calculated; the pressure drop across the total length must also be estimated [8,18] .

190 The outlet column volumetric flow ($F_{o(c)}$) can be derived by the Poiseulle equation (Eq. 1)

191

$$192 \quad F_{o(c)} = \frac{60\pi r^4 (p_i^2 - p_o^2) T_{ref}}{16\eta L p_o T} \quad \text{Equation 1}$$

193

194 where r is the column radius, η the dynamic viscosity of the carrier gas at a given temperature, L is the
195 column length, p_i and p_o are the absolute inlet and outlet pressures, and T_{ref} is the reference temperature
196 (typically 298K) and T is the absolute operative temperature.

197 The pressure at any point (z) along the column can be calculated according to Equation 2:

198

$$199 \quad p_z = \sqrt{p^2 - \left(\frac{z}{L}\right) (p^2 - 1)} \quad \text{Equation 2}$$

200

201 The linear velocity at the column outlet (u_o) is:

202

$$203 \quad u_o = \left(\frac{r^4 (p_i^2 - p_o^2)}{16\eta L p_o} \right) \quad \text{Equation 3}$$

204

205 where r is the column radius, η the dynamic viscosity of the carrier gas at the operating temperature, L is
206 the column length, p_i and p_o are the absolute inlet and outlet pressures. The average velocity is proportional
207 to the outlet velocity corrected by the compression factor j :

$$208 \quad \bar{u} = u_o \cdot j \quad \text{Equation 4}$$

209 where

$$210 \quad j = \frac{3(p^2 - 1)}{2(p^3 - 1)} \quad \text{Equation 5}$$

211

212 The average linear velocity along each separation dimension can be estimated by combining the above
213 functions. **Table 1** reports average linear velocities, calculated at 333 K (60°C), together with inlet pressure
214 (p_i), midpoint pressure (p_2) at the connection between primary and secondary column(s) in kPa (over
215 pressure) and hold-up times (s). In the case of *Set-up II*, the data do not include the adjustment of outlet
216 pressure by the auxiliary flow controller.

217

218 **3.2 Parallel dual secondary columns operating at different outlet pressures (GC×2GC-MS/FID)**

219 The first part of this study was carried out on dual parallel columns of identical inner diameter (i.e., 0.10
220 mm d_c) but of an almost equivalent length in terms of flow resistance. *Set-up I* was inspired by the “split-
221 flow” configuration proposed by Tranchida *et al.* [17], with the sole difference that the outlet of the split
222 capillary (an OV1701 capillary column with 0.10 μm d_f) was connected to a FID detector (atmospheric
223 pressure). Compared to a conventional configuration (*Set-up III*), where one of the two dimensions has to
224 operate very far from its optimum performance, whatever the head pressure, in *Set-up I* close-to-optimal
225 linear velocities in both chromatographic dimensions are applied, i.e. ^1D at about 34 cm/s and the ^2Ds at
226 about 180 cm/s (see **Table 1**).

227 Differences in secondary column length were expected to condition the separation in terms of absolute
228 retention and peak-widths. However, the resulting 2D patterns were expected to be consistent, although
229 not identical. According to Schutjes *et al.* [21], who rearranged the *Golay* plate height equation in terms of
230 dimensionless parameters (i.e., $\xi = H/H_{min}$ and $v = \bar{u}/\bar{u}_{opt}$), operating at $p_i/p_o \gg 1$ (i.e., vacuum outlet), the
231 maximum efficiency is reached for a close interval of average linear velocities around \bar{u}_{opt} . Conversely, when
232 p_i/p_o approaches unity (i.e. at ambient pressure), the experimental curve of H/H_{min} as a function of \bar{u}/\bar{u}_{opt} is
233 flatter, and enables a better separation efficiency. With *Set-up I* lower efficiencies were expected for the
234 MS branch [21] also in consequence of the longitudinal diffusion effect.

235 The experimental results confirmed these hypotheses: **Figure 1** shows the raw chromatogram overlaid with
236 2D plots of linear hydrocarbons from C13 to C15 analyzed in isothermal conditions (i.e., 150°C) at 296 kPa
237 head-pressure with *Set-ups I* and *II*. System hold-up times, measured experimentally with methane
238 injections at 80% of MFC cold jet regulation, were 1.905 min and 0.86 s in the ^1D and ^2D respectively, in fair
239 accordance with the expected values. Alkanes showed an absolute retention time shift (MS vs. FID) of -0.18
240 s for n-C13 and of -0.36 s for n-C15. Although minimized by the lower retention in the second dimension
241 due to the temperature of the isothermal analysis, a much larger mismatch was expected for temperature
242 programmed conditions and strongly retained analytes.

243 **Figure 2** reports 2D plots (**Fig. 2a** full scan MS and **Fig. 2b** FID plots) of *Artemisia umbelliformis* essential oil,
244 analyzed with *Set-up I*. The consistency of the 2D patterns of the two detectors is evident; the structured
245 patterns of mono-terpenoid (*m*) and sesqui-terpenoid (*s*) hydrocarbons are clearly organized, and
246 separated from the oxygenated derivatives (*mox* and *sox*) and from other secondary metabolites (mono
247 terpenoid esters - *mest*). More polar compounds (carbonyl derivatives, alcohols and esters) having greater
248 affinity for the second dimension stationary phase were more strongly retained along the ^2D branch
249 towards MS (higher retention factors - *k*).

250 The magnitude of the retention time shift is better illustrated in **Figures 3a** and **3b**, which show ^2D retention
251 time absolute differences (FID vs. MS) for: (**3a**) *n-alkane* hydrocarbons from *n*-C9 to *n*-C25 and (**3b**)
252 fourteen volatiles of interest in flavor and fragrance applications. For the *n*-alkanes, where retention in the
253 ^2D is negligible, absolute differences in retention times in no case exceeded (-)0.15 s (i.e., 3% as relative %

254 difference over 5 seconds of ²D separation time); conversely, ²D retention shifts for more polar compounds
255 (**Fig. 3b**) were larger with differences between MS and FID patterns ranging from the (-)0.12 s of α -pinene
256 to the (-) 0.68 s of vanillin (i.e., 2.38 and 13.6 % of relative difference). Marked differences were recorded
257 for the more polar analytes (benzyl alcohol, cinnamyl alcohol, vanillin, isoeugenol and isoeugenyl acetate)
258 that suffered from the wrap-around phenomenon.

259

260 **3.3 Parallel dual secondary columns operating at equivalent (atmospheric) outlet pressures (GC \times 2GC- 261 MS/FID)**

262 The study continued, adopting two secondary columns with the same number of theoretical plates and the
263 same equivalent lengths, in terms of flow resistance; in addition a correction of the pressure drop across
264 dimensions was operated by an auxiliary flow/pressure controller (EPC) connected to a microfluidic device
265 installed between the outlet of the ²D_{MS} column and the MS transfer line (restrictor) [18].

266 In *Set-up II*, the two ²D columns were both 1.4 meters long (0.6 meters at the head of each column were
267 wrapped to form the modulation loop) thus leaving available 0.8 meters of each column for separation. At
268 the end of the ²D to MS, 0.17 m x 0.1 mm d_c of deactivated silica capillary (restrictor) was used to
269 compensate for differences in flow resistance (**Table 1: Set-up II - auxiliary off conditions**). Additional
270 helium flow was delivered by setting the auxiliary EPC at 40 kPa (5.7 psi relative) to adjust the outlet
271 pressure towards MS. The compensation was minimal, because of the low resistance of the two parallel
272 ²Ds.

273 The outlet pressure correctness was verified by isothermal analysis (i.e., 150°C) of linear hydrocarbons from
274 C13 to C15 at 296 kPa head-pressure; **Figure 1b** shows the raw chromatograms overlaid with the FID ²D plot
275 resulting from an outlet pressure correction towards MS of 40 kPa. System hold-up times were 1.91 min
276 and 0.88 s in the ¹D and ²D respectively. Alkanes did not show any retention time shift. Experiments
277 without outlet pressure correction were also run with test mixtures and under programmed temperature
278 conditions; the relative difference between ²D retention times was on average 0.6 % for *n*-alkanes and 5.65
279 % for the FFStd2 model mixture. Figures **3c** and **3d** show absolute differences in time values in detail. Again,
280 wrapped-around analytes showed higher discrepancies between ²D elution times, due to accumulation of
281 the delay error across subsequent modulations. However, with pressure compensation, the retention shift
282 in no case exceeded 1.1 % for linear hydrocarbons and 4% (cinnamyl alcohol) for the FFStd2 model mixture
283 components. These values are in agreement with those reported by Shellie *et al.* [18], although most of the
284 analytes investigated in that study had lower retention in both dimensions.

285 **Figures 2c** and **2d** show the 2D plots (**Fig. 2c** full scan MS and **Fig. 2d** FID plot) of *Artemisia umbelliformis*
286 essential oil, analyzed with *Set-up II* with auxiliary outlet compensation. As is clear, the 2D patterns are in
287 this setup highly consistent, the structure is maintained, and the chromatographic space properly occupied.
288 Experiments run without any outlet pressure correction (data not shown) produced 2D patterns with very

289 few differences from those shown, and this approach would be a good alternative when an additional EPC
290 is not available, or turbo pumping systems do not tolerate high outlet flows. In such cases, adaptive
291 algorithms (called *transforms*) for pattern recognition, like those used for template matching procedures
292 [23] in targeted and untargeted data elaboration, can successfully compensate for ²D retention times shifts,
293 and consistently transfer identification from MS to FID.

294 295 **3.4 Single secondary column with dual parallel detection (GC×GC-MS/FID)**

296 To evaluate the practical advantages that can be obtained by operating at near-optimal linear velocities,
297 with two parallel columns and two detection systems, an additional setup (*Set-up III*) consisting of a single
298 ²D column (1.4 m x 0.1 mm d_c) connected to two parallel detectors was tested. Pressure/flow conditions
299 adopted were a compromise between optimal conditions in both dimensions, and were allowed to run at
300 23 cm/s and 240 cm/s in the ¹D and in the ²D, respectively. As expected, with *Set-up III* ¹D retention times
301 slightly increased, reflecting the higher elution temperatures that resulted, while those in the ²D decreased,
302 due to the consequent loss of retention. **Figures 4a, 4b** and **4d** show differences in retention times from
303 *Set-up I* to *Set-up III*.

304 For *Artemisia umbelliformis* essential oil, although the separation structure was maintained, the overall
305 resolution was lower. **Figures 2e** and **2f** show the 2D patterns resulting from *Set-up III*. In this case, a
306 concurrent reduction of the temperature rate and of the modulation period might be expected to produce
307 better results, although analysis time is longer.

308 309 **3.5 Practical advantages of the optimized GC×2GC-MS/FID platform**

310 Some aspects deserve a brief discussion, to outline the practical advantages on real-world samples deriving
311 from a GC×2GC-MS/FID platform, in terms of both dual ²D column and dual detection. *Artemisia*
312 *umbelliformis* essential oil was selected as a case study, since its detailed quantitative profiling is interesting
313 for botanical classification, as well as in the light of quality aspects relating to its use to prepare a highly-
314 prized Alpine liqueur, called “genepi”, characterized by a bitter taste and a distinctive aroma [24]. These
315 sensory properties can be ascribed to terpenoids, in particular to α - and β -thujones, the main components
316 of the volatile fraction for the aroma profile, and to sesquiterpene lactones with a *cis*-eudesmanolide
317 skeleton (5-desoxy-5-hydroperoxy-5-epitelekin; 5-desoxy-5-hydroperoxytelekin and umbellifolide) for its
318 bitterness [25]. The debate on the toxicity of thujones is still open [26], and European Union legislation has
319 fixed a limit of 35 mg/kg on the total amount of these compounds in alcoholic beverages [27]. Thujone-free
320 chemotypes of *A. umbelliformis* have been selectively bred to overcome this issue, and diagnostic
321 fingerprints have been defined by combining biomolecular characterization with chemical profiling of
322 informative secondary metabolites [25]. In any case, a detailed profiling of the volatile fraction is necessary
323 to assess both sensory quality and safety of the aerial parts that are used to prepare the liqueur.

324 The first aspect to be considered is the separation power of GC×2GC-MS/FID. Resolution reflects the
325 adequacy of the separation conditions adopted for a given group of target analytes, and becomes
326 fundamental for samples where several informative peaks in variable abundances elute in a given region of
327 the chromatographic space. Extra-chromatographic phenomena, e.g. column overloading, may in these
328 cases condition correct separation, i.e. identification/quantitation. For example, when ²D overloading
329 occurs, minor peaks eluting in the proximity of highly abundant components, with large peak-width, may be
330 lost, together with the information they carry. The ²D dual column doubles the ²D loadability, thus limiting
331 ²D overloading and loss of significant minor peaks due to this phenomenon. At the same time, the higher
332 efficiency due to the average linear velocity closer to the optimal value, and the enhanced ²D stationary
333 phase selectivity, increase the system orthogonality, improving occupation of the chromatographic plane.
334 For instance, the calculated α-thujone half-height peak width in the FFStd2 model mixture at 100 mg/L, was
335 120 ms (see **Table 2**). In *A. umbelliformis* essential oil, α- and β-thujones are the two most abundant peaks,
336 each with a peak width of 480 ms, that dramatically overloads the ²D; in *Set-up III*, where the second
337 dimension loadability is halved compared to *Set-up II*, they coelute in ¹D-GC with two minor components,
338 i.e. nonanal and 2-methylbutyl isovalerate. Apparent resolution values (*R*) estimated on the raw
339 chromatogram, and referred to the most abundant modulation for all compounds, were 1.93 for the 2-
340 methylbutyl isovalerate/α-thujone pair with *Set-up II*, and 1.53 with *Set-up III*, while for the nonanal/α-
341 thujone pair they were 1.28 for *Set-up II*, but coeluted in *Set-up III* (**Figure 5**).

342 A second practical aspect to consider for in attempting an overall evaluation of the potential of a GC×2GC-
343 MS/FID system concerns quantitation reliability: this exploits the synergisms of dual detection operating by
344 different principles. MS is known to provide a fundamental contribution to unequivocal analyte
345 identification, while FID offers a wide dynamic range of linearity and a very high frequency of acquisition,
346 thereby improving the accuracy of 2D peak (areas) volumes. Moreover, the correct alignment of the two
347 patterns obtained with both *Setup II* and *Setup III* enables one to consider the data set from the two
348 detectors as a single integrated system, thus cross-validating the results. These considerations are
349 confirmed by experimental data on the FFStd2 mixture. **Table 2** shows ¹D and ²D retention times and their
350 absolute errors (²D Error in seconds), Normalized 2D Volumes for MS (TIC current) and FID signals
351 (normalization was done on geranyl acetate), half-height peak-width (50% peak width (ms)) and the
352 number of points per peak (MS operated at 28 Hz and FID at 150 Hz) for the analytes of FFStd2 mixture
353 with *Set-up II* and *Set-up III*.

354 These results demonstrate that the chromatographic efficiency (expressed as half-height peak-width) is
355 comparable for the two setups. It has to be stressed that *Set-up III* had to operate at ²D flow conditions
356 close to those adopted for the two-parallel-column system; if higher head-pressures had been applied,
357 peak-widths would have been narrower. The number of points-per-peak was, in consequence, similar for

358 *Setup II* and *Setup III* for each detector, while mass quantitative descriptors (Normalized 2D Volumes) from
359 the two detectors were consistent.

360 However, the potential of dual detection can concretely be perceived with real-world samples (e.g. *A.*
361 *umbelliformis* essential oil). In these applications, the consistency of acquired MS spectra is fundamental
362 since identification is mainly based on commercial spectral libraries. **Table 3** reports the ¹D Linear Retention
363 Indices (experimental and reference values [28]), the MS match factors resulting from the NIST Identity
364 Spectrum Search algorithm (NIST MS Search 2.0 ver. d) on spectra collected in commercial databases,
365 and/or on spectra obtained by analyzing reference compounds, and the Signal-to-Noise (Peak-to-Peak S/N
366 as calculated by the Agilent algorithm - SNR) estimated on the highest modulation of each 2D peak of the
367 components characterizing *A. umbelliformis* essential oil.

368 For the selected analytes, the quality of the spectral match, as well as the S/N values were comparable
369 between *Set-up II* and *III*. Higher S/N values would be expected for a conventional configuration, because of
370 the sharper peaks generated at faster flow rates. Moreover, within the experimental conditions applied
371 here, the ²D peak widths generated were comparable (**Table 2**) and in accordance with the results recently
372 obtained by Tranchida *et al.* [29].

373 Data reported in **Table 3** also show that the GC×2GC-MS/FID platform provides enhanced information,
374 because the concurrent presence of two detectors not only provides contemporary analyte identification
375 and quantitation, but also offers internal cross-validation of results. It is also important to note that the
376 international guidelines for quantitative gas chromatography of volatile flavoring substances and essential
377 oils [30-32] indicate Relative Response Factors (*RRF*) (i.e. external standard calibration with internal
378 standard normalization) as the most suitable approach to obtain consistent quantitative data in these
379 matrices, in particular with MS detection. However, for complex samples consisting of hundreds of
380 potentially informative peaks, a full quantitative assessment by *RRFs* cannot be applied in practice. The
381 internal normalization approach performed on the FID signal, also known as analyte percent normalization
382 [31], is therefore accepted. In this case, the composition error is minimized by an appropriate selection of
383 internal standard(s) and FID response factors [33-35] making true quantitation by *RRF* necessary only for
384 those compounds that are limited by law (e.g. α - and β -thujone). FID also opens the possibility of applying
385 the approach introduced by de Saint Laumer *et al.* [36] where analytes' *RRFs* on FID signal are estimated on
386 the basis of combustion enthalpies. With this approach, target analytes can be quantified through
387 estimated *RRFs*, with accuracy errors limited to a few % points even without external standard calibration.
388 Parallel dual detection thus seems to be very promising for reliable and simple qualitative component
389 identification, and to quantitate markers of complex samples of natural origin.

390

391 **4. Conclusions**

392 The advantages of using a dual-secondary-column dual-detection system in an integrated platform for
393 GC×GC have been discussed, and some practical aspects concerning the tuning of experimental conditions
394 to obtain consistent separation patterns from both dimensions have been addressed. These systems can
395 operate at close-to-optimal ²D linear velocities, and double the secondary column loading capacity, with
396 positive effects on overall system orthogonality and resolution.

397 Experimental data also indicate that the GC×2GC-MS/FID system provides consistent results, both in terms
398 of analyte identification (reliability of spectra and MS matching) and quantitation, also affording internal
399 cross-validation of quantitation accuracy.

400 The choice of different setups, in terms of ²D column dimensions and flow conditions, should take into
401 consideration some critical aspects, including the auxiliary flow correction, which should be compatible
402 with the turbo pumping capacity and the required sensitivity. The outlet pressure correction adopted in the
403 present study was minimal, and compatible with both system-limiting factors.

404 These data open the way to investigating further applications, where system orthogonality and loading
405 capacity are key-factors for successful separations.

406

407 **Acknowledgements**

408 This study was supported by Ricerca Finanziata da Università - Fondo per la Ricerca Locale (Ex 60%) Anno
409 2013.

410

411

412 **References**

- 413 1. M. Adahchour, J. Beens, R.J.J. Vreuls, U.A.Th. Brinkman, Recent developments in comprehensive
414 two-dimensional gas chromatography (GC × GC): I. Introduction and instrumental set-up, Trends
415 Anal. Chem. 25 (2006) 438-454.
- 416 2. H.J. Cortes, B. Winniford, J. Luong, M. Pursch, Comprehensive two dimensional gas
417 chromatography review, J. Sep. Sci. 32 (2009) 883-904.
- 418 3. C. Cordero, E. Liberto, C. Bicchi, P. Rubiolo, P. Schieberle, S.E. Reichenbach, Q. Tao, Profiling food
419 volatiles by comprehensive two-dimensional gas chromatography coupled with mass spectrometry:
420 Advanced fingerprinting approaches for comparative analysis of the volatile fraction of roasted
421 hazelnuts (*Corylus avellana* L.) from different origins, J. Chromatogr. A. 1217(2010) 5848-5858
- 422 4. J. Harynuk, T. Górecki, J. de Zeeuw, Overloading of the second-dimension column in comprehensive
423 two-dimensional gas chromatography, J. Chromatogr. A. 1071 (2005) 21-27
- 424 5. Z. Zhu, J. Harynuk, T. Górecki, The Effect of the First-dimension Column Film Thickness on
425 Comprehensive Two-dimensional Gas Chromatographic Separation, J. Chromatogr. A. 1105 (2006)
426 17-24
- 427 6. Z. Liu, J. B. Phillips, Comprehensive two-dimensional gas chromatography using an on-column
428 thermal modulator interface, J. Chromatogr. Sci. 1067 (1991) 227-231
- 429 7. J. B. Phillips, C. J. Venkatramani, Comprehensive two-dimensional gas chromatography applied to
430 the analysis of complex mixtures, J. Microcolumn Sep. 5 (1993) 511-516
- 431 8. P. Q. Tranchida, A. Casilli, P. Dugo, G. Dugo, L. Mondello, Generation of improved gas linear
432 velocities in a comprehensive two-dimensional gas chromatography system, Anal. Chem. 79 (2007)
433 2266-2275
- 434 9. J. Harynuk, T. Gorecki, Comprehensive two-dimensional gas chromatography in stop-flow mode, J.
435 Sep. Sci. 27 (2004) 431-441.
- 436 10. J. Harynuk, T. Gorecki, Comparison of comprehensive two-dimensional gas chromatography in
437 conventional and stop-flow modes, J. Chromatogr. A 1105 (2006) 159-167.
- 438 11. N. Oldridge, O. Panic, T. Gorecki, Stop-flow comprehensive two-dimensional gas chromatography
439 with pneumatic switching, J. Sep. Sci. 31 (2008) 3375-3384.
- 440 12. M. M. Koek, B. Muilwijk, L.L.P. van Stee, T. Hankemeier, Higher mass loadability in comprehensive
441 two-dimensional gas chromatography-mass spectrometry for improved analytical performance in
442 metabolomics analysis, J. Chromatogr. A. 1186 (2008) 420-429
- 443 13. C. Cordero, C. Bicchi, M. Galli, S. Galli, P. Rubiolo, Evaluation of different internal-diameter column
444 combinations in comprehensive two-dimensional gas chromatography in flavour and fragrance
445 analysis, J. Sep. Sci. 31 (2008) 3437-3450

- 446 14. D. Peroni, R.J. Vonk, W. van Egmond, H.-G. Janssen, Macroporous polymer monoliths as second
447 dimension columns in comprehensive two-dimensional gas chromatography: a feasibility study, J.
448 Chromatogr. A 1268 (2012) 139-149
- 449 15. D. Peroni, A.A.S. Sampat, W. van Egmond, S. de Koning, J. Cochran, R. Lautamo, H.-G. Janssen,
450 Comprehensive two-dimensional gas chromatography with a multi-capillary second dimension: A
451 new column-set format for simultaneous optimum linear velocity operation, J. Chromatogr. A 1317
452 (2013) 3-11
- 453 16. D. Peroni, H.-G. Janssen, Comprehensive two-dimensional gas chromatography under high outlet
454 pressure conditions: a new approach to correct the flow-mismatch issue in the two dimensions,
455 Journal of Chromatography A, 1332 (2014) 57–63
- 456 17. P.Q. Tranchida, M. Zoccali, F.A. Franchina, A. Cotroneo, P. Dugo, L. Mondello, Gas velocity at the
457 point of re-injection: an additional parameter in comprehensive two-dimensional gas
458 chromatography optimization, J. Chromatogr. A. 1314 (2013) 216-223
- 459 18. R. Shellie, P. Marriott, P. Morrison, L. Mondello, Effects of pressure drop on absolute retention
460 matching in comprehensive two-dimensional gas chromatography, J. Sep. Sci. 27 (2004) 504-512
- 461 19. European Directorate for the Quality of Medicines (EDQM). European Pharmacopoeia VIII ed. 2014
- 462 20. C. Bicchi, G. M. Nano, C. Frattini, On the composition of the essential oils of *Artemisia genepi* Weber
463 and *Artemisia umbelliformis* Lam., Z. Lebensm. Unters. Forsch. 175 (1982) 182-185
- 464 21. J. Beens, H. G. Janssen, M. Adahchour, U. A. Th. Brinkman, Flow regime at ambient outlet pressure
465 and its influence in comprehensive two-dimensional gas chromatography, J. Chromatogr. A. 1086
466 (2005) 141-150
- 467 22. C. Schutjes, P. Leclercq, J. Rijks, C. Cramers, C. Vidalmadjar, G. Guiochon, Model describing the role
468 of the pressure gradient on efficiency and speed of analysis in capillary gas chromatography, J.
469 Chromatogr. 289 (1984) 163-170
- 470 23. S.E. Reichenbach, X. Tian, C. Cordero, Q. Tao, Features for non-targeted cross-sample analysis with
471 comprehensive two-dimensional chromatography, J. Chromatogr. A 1226 (2012) 140- 148
- 472 24. M. Mucciarelli, M. Maffei, Introduction to the genus. In Medicinal and Aromatic Plants—Industrial
473 Profiles: Artemisia; Wright, C. W., Ed.; Taylor and Francis: London, U.K., 2002; pp 1– 50. Open URL
474 UNIV STUDI DI TORINO
- 475 25. P. Rubiolo, M. Matteodo, C. Bicchi, G. Appendino, G. Gnani, C. Berteà, M. Maffei, Chemical and
476 Biomolecular Characterization of *Artemisia umbelliformis* Lam., an Important Ingredient of the
477 Alpine Liqueur “Genepi” J. Agric. Food Chem., 57 (2009) 3436-3443
- 478 26. D. W. Lachenmeier, D. Nathan-Maister, T. A. Breaux, E. M. Sohnius, K. Schoeberl, T. Kuballa,
479 Chemical composition of vintage preban absinthe with special reference to thujone, fenchone,

- 480 pinocamphone, methanol, copper, and antimony concentrations, *J. Agric. Food Chem.* 56 (2008)
481 3073-3081
- 482 27. Council Directive (EC) No 1334/2008 on on flavourings and certain food ingredients with flavouring
483 properties for use in and on foods and amending Council Regulation (EEC) No 1601/91, Regulations
484 (EC) No 2232/96 and (EC) No 110/2008 and Directive 2000/13/EC.
- 485 28. Robert P. Adams, *Identification of Essential Oil Components by Gas Chromatography/Mass*
486 *Spectrometry*, 4th Edition, Allured books
- 487 29. P.Q. Tranchida, M. Zoccali, F.A. Franchina, P. Dugo, L. Mondello, Measurement of fundamental
488 chromatography parameters in conventional and split-flow comprehensive two-dimensional gas
489 chromatography-mass spectrometry: A focus on the importance of second-dimension injection
490 efficiency, *J Sep. Sci.* 36 (2013) 212-218
- 491 30. IOFI. Analytical procedure for a general quantitative method using coupled capillary gas
492 chromatography/mass spectrometry with selected ion monitoring (SIM). *Z. Lebensm.-Unters.-*
493 *Forsch.* 1997, 204, 395.
- 494 31. ISO. Essential oils – Analysis by gas chromatography on capillary columns – General methods.
495 International standard ISO 7609, International Organization for Standardization, Geneva, 1985
- 496 32. Recommended Practice Flavour *Fragr. J.* 26 (2011) 297
- 497 33. R. Costa, M.R. De Fina, M.R. Valentino, A. Rustaiyan, P. Dugo, G. Dugo, An investigation on the
498 volatile composition of some *Artemisia* species from Iran, *Flavour Fragr. J.* 24 (2009) 75-82
- 499 34. C. Bicchi, E. Liberto, M. Matteodo, B. Sgorbini, L. Mondello, B. d'Acampora Zellner, Quantitative
500 analysis of essential oils: a complex task, *Flavour Fragr. J.* 23 (2008) 382-391
- 501 35. R. Costa, B. d'Acampora Zellner, M. L. Crupi, M. R. De Fina, M. R. Valentino, P. Dugo, G. Dugo, L.
502 Mondello, GC-MS, GC-O and enantio-GC investigation of the essential oil of *Tarhonanthus*
503 *camphoratus* L., *Flavour Fragr. J.*, 23 (2008) 40-48
- 504 36. J.Y. de Saint Laumer, E. Cicchetti, P. Merle, J. Egger, A. Chaintreau, Quantification in Gas
505 Chromatography: Prediction of Flame Ionization Detector Response Factors from Combustion
506 Enthalpies and Molecular Structures, *Anal. Chem.* 82 (2010) 6457-6462

507

508 **Caption to Figures**

509 **Figure 1:** 2D plots (upper part) and raw chromatograms of *n*-C13-*n*-C15 linear hydrocarbons, analyzed in
510 isothermal conditions at 150°C, 296 kPa head-pressure and 5s of modulation period. **1a:** *Set-up I*; **1b:** *Set-up*
511 *II* with the outlet pressure correction as indicated in the text.

512

513 **Figure 2:** 2D plots of *Artemisia umbelliformis* essential oil, analyzed with *Set-up I* (**2a** full scan MS and **2b** FID
514 signals), *Set-up II* (**2c** full scan MS and **2d** FID signals) and *Set-up III* (**2e** full scan MS and **2f** FID signals).
515 Chemical classes: *m*: mono-terpene hydrocarbons, *s*: sesqui-terpenene hydrocabons, *mox*: oxygenated
516 monoterpenoids, *sox*: oxygenated sesquiterpenoids, *mest*: mono terpenoid esters.

517

518 **Figure 3:** ²D retention time absolute differences (FID vs. MS) for: **3a:** *n*-alkanes from *n*-C9 to *n*-C25, **3b:**
519 fourteen volatiles of interest for the flavor and fragrance field.

520

521 **Figure 4:** ¹D (**4a**) and ²D (**4b**) retention time variations for *Set-up I*, *Set-up II* (with and without outlet
522 pressure correction) and *Set-up III*.

523

524 **Figure 5:** 2D plots of *Artemisia umbelliformis* essential oil, the magnified region corresponds to the elution
525 area of 2-methylbutyl isovalerate, nonanal and α -thujone. **5a:** the separation pattern obtained from *Set-up*
526 *II*, and the corresponding raw chromatogram, **5b:** *Set-up III* separation. Apparent resolution values are
527 reported in the text.

528

529 **Caption to Tables**

530 **Table 1:** Column configurations, column head pressure (p_i) and midpoint pressure (i.e., estimated pressure
531 at the junction between the 1D column and the two secondary columns - p_2), estimated linear velocities in
532 the 1D and two 2Ds ($^1\bar{u}$, $^2\bar{u}_{MS}$, $^2\bar{u}_{FID}$), hold-up times and calculated split-ratio.

533
534 **Table 2:** 1D (min) and 2D (sec) retention times, 2D absolute errors (sec), half-height peak-width (ms),
535 number of scans/points per (modulated) peak, normalized 2D Volumes (normalization on geranyl acetate)
536 obtained by analyzing the FFStd2 model mixture with *Set-up II* and *Set-up III*.

537
538 **Table 3:** *Artemisia umbelliformis* essential oil target analytes listed, together with experimental and
539 tabulated [28] Linear Retention Indices in the 1D (I_s^T), MS match factors resulting from the NIST Identity
540 Spectrum Search algorithm, Signal-to-Noise values (Peak-to-Peak S/N as calculated by the Agilent algorithm
541 - SNR) estimated on the highest modulation of each 2D peak, Normalized 2D Volumes (normalization was
542 done on the Internal Standard n-C12) for *Set-ups II* and *III*.

543

Table 1

	¹ D column	² D column(s)	Carrier gas (He) ^a	Auxiliary EPC correction
Set-up I	30 m, 0.25 mm d _c , 0.25 μm d _f SE52 (95% polydimethylsiloxane, 5% phenyl) Mega (Legnano, Milan, Italy)	to MS detector: 1.6 m - to FID detector: 1.4 m column dimensions: 0.1 mm d _c , 0.10 μm d _f OV1701 (86% polydimethylsiloxane, 7% phenyl, 7% cyanopropyl) Mega (Legnano, Milan, Italy)	p_1 : 296.0 KPa p_2 : 182.6 KPa $^1\bar{u}$: 34.3 cm/s $^2\bar{u}_{MS}$: 195 - hold-up: 0.8 s $^2\bar{u}_{FID}$: 178 - hold-up: 0.8 s split ratio (MS/FID): 50:50	
Set-up II	30 m, 0.25 mm d _c , 0.25 μm d _f SE52 (95% polydimethylsiloxane, 5% phenyl) Mega (Legnano, Milan, Italy)	to MS detector: 1.4 m - to FID detector: 1.4 m column dimensions: 0.1 mm d _c , 0.10 μm d _f OV1701 (86% polydimethylsiloxane, 7% phenyl, 7% cyanopropyl) deactivated capillary to MS detector: 0.17 m, 0.1 mm d _c Mega (Legnano, Milan, Italy)	p_1 : 296.0 KPa p_2 : 181.9 KPa p_{aux} : Off $^1\bar{u}$: 34.5 cm/s $^2\bar{u}_{MS}$: 198 - hold-up: 0.8 s $^2\bar{u}_{FID}$: 177 - hold-up: 0.8 s split ratio (MS/FID): 51:49	p_1 : 296.0 KPa p_2 : 182.6 KPa p_{aux} : 39.9 KPa (relative) $^1\bar{u}$: 34.2 cm/s $^2\bar{u}_{MS}$: 180 - hold-up: 0.8 s $^2\bar{u}_{FID}$: 180 - hold-up: 0.8 s split ratio (MS/FID): 50:50
Set-up III	30 m, 0.25 mm d _c , 0.25 μm d _f SE52 (95% polydimethylsiloxane, 5% phenyl) Mega (Legnano, Milan, Italy)	column dimensions: 1.4 m, 0.1 mm d _c , 0.10 μm d _f OV1701 (86% polydimethylsiloxane, 7% phenyl, 7% cyanopropyl) deactivated capillaries for effluent splitting to parallel detectors: to MS detector: 0.4 m, 0.1 mm d _c - to FID detector: 0.25 m, 0.1 mm d _c Mega (Legnano, Milan, Italy)	p_1 : 280.0 KPa p_2 : 205.1 KPa $^1\bar{u}$: 22.8 cm/s $^2\bar{u}$: 240 - hold-up: 0.6 s split ratio (MS/FID): 50:50	

^a: reported values were calculated on the basis of reference equations and are just approximations of real ones

Table 2

Compound Name	<i>Set-up II</i>						<i>Set-up III</i>										
	MS (TIC signal)			FID signal			MS (TIC signal)			FID signal							
	¹ D (min)	² D (sec)	² D Error (sec)	Half height pw (ms)	Number of scans	Norm 2D Volume	Half height pw (ms)	Points per peak	Norm 2D Volume	¹ D (min)	² D (sec)	Half height pw (ms)	Number of scans	Norm 2D Volume	Half height pw (ms)	Points per peak	Norm 2D Volume
α-Pinene	8.25	1.58	0.04	60	21	1.468	60	144	1.358	11.92	1.27	60	14	1.36	60	79	1.153
Benzaldehyde	9.34	2.61	0.02	120	19	0.757	60	89	0.898	13.17	2.02	120	15	0.462	60	115	0.563
Benzyl Alcohol	12.34	3.71	-0.02	180	27	0.424	120	162	0.860	16.42	2.78	180	23	0.428	120	158	0.726
α-Thujone	15.42	2.68	0.00	120	27	0.993	60	113	1.002	19.84	2.02	120	21	0.871	120	86	0.903
Camphor	17.25	2.86	-0.01	120	20	1.400	120	162	1.280	21.84	2.10	120	16	1.160	120	99	1.152
Carvone	21.75	3.05	-0.02	120	23	0.543	120	207	0.801	26.34	2.26	120	19	0.535	120	115	0.707
Cinnamyl Alcohol	24.84	4.10	-0.20	180	27	0.070	120	297	0.473	29.17	2.86	180	26	0.057	120	252	0.379
<i>Geranyl acetate</i>	27.67	2.57	-0.04	120	30	1.000	60	126	1.000	32.17	1.90	120	29	1.000	60	86	1.000
Vanillin	28.50	4.81	-0.13	180	25	0.155	180	207	0.831	33.09	3.45	240	31	0.126	180	209	0.551
Coumarin	30.09	4.62	-0.18	180	33	0.241	120	144	0.823	34.92	3.33	240	29	0.187	120	187	0.541
Isoeugenol	30.59	3.57	-0.12	120	23	0.372	120	279	0.809	35.25	2.54	180	36	0.256	120	125	0.716
Isoeugenyl acetate	36.92	3.71	-0.11	120	21	0.481	120	225	0.693	41.5	2.66	120	21	0.438	120	101	0.791
Benzyl Benzoate	42.75	3.12	0.02	120	56	0.475	120	234	0.710	47.59	2.42	180	29	0.425	120	259	0.799
Sclareol	57.09	3.40	-0.01	180	41	0.828	120	153	1.273	61.92	2.62	240	31	0.530	120	145	1.179

Table 3

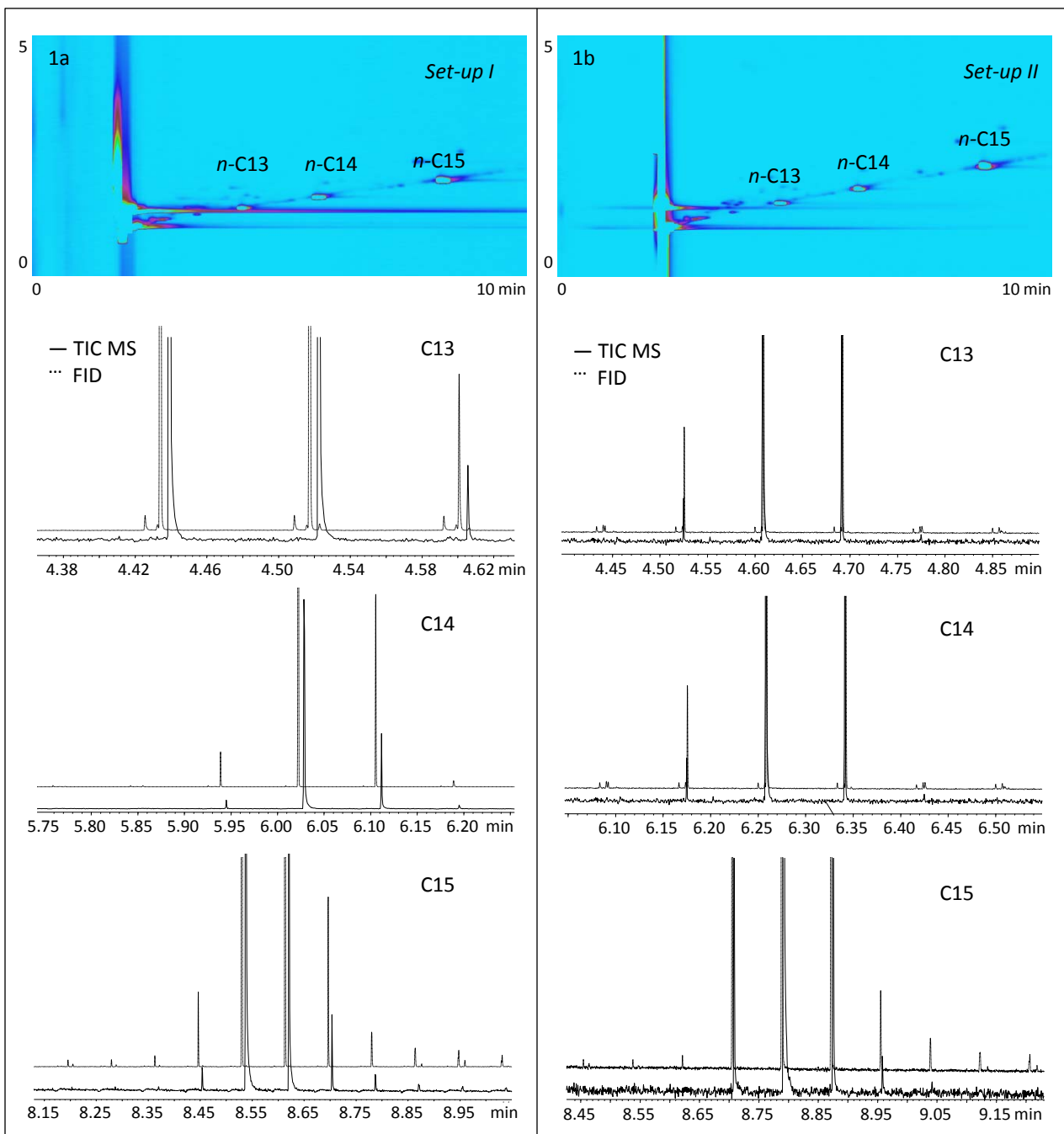
#ID	Compound Name	Exp. I_s^T	Ref. I_s^T ^a	Set-up II		Set-up III		Set-up II	Set-up III	Set-up II	Set-up III
				MS Match Factor	SNR	MS Match Factor	SNR	Norm 2D Volume MS (TIC) signal	Norm 2D Volume FID signal	Set-up II	Set-up III
1	Thujene	918	931	884	3740	906	3433	0.452	0.552	0.242	0.249
2	α -Pinene	925	939	860	12791	833	12232	0.542	0.746	0.666	0.679
3	Camphene	941	953	909	4170	913	3828	0.910	0.978	0.356	0.367
4	Sabinene	966	976	874	63223	893	53153	5.757	5.830	3.477	3.548
5	β -Pinene	970	980	892	44034	889	40563	9.521	9.150	4.063	4.190
6	β -Myrcene	984	991	905	10080	901	9252	2.023	2.185	0.802	0.825
7	p-Cymene	1021	1026	917	59306	915	49859	12.652	15.281	6.166	6.358
8	Limonene	1025	1031	913	3965	927	3640	0.472	0.509	0.271	0.280
9	1,8-Cineole	1029	1033	907	88187	892	84336	47.829	51.810	19.558	20.169
10	γ -Terpinene	1056	1062	853	17482	875	16046	1.900	2.856	1.513	2.259
11	cis-Sabinenehydrate	1067	1068	883	9225	869	7755	2.282	3.878	1.654	1.706
12	α -Terpinolene	1085	1088	865	4416	870	4054	0.750	0.861	0.475	0.489
13	2-Methylbutyl isovalerate	1111	1109	912	1264	-	-	0.001	-	0.367	-
14	α -Thujone	1111	1102	903	63176	890	57988	452.460	482.096	157.457	160.677
15	Nonanal	1113	1098	881	1409	-	-	0.193	-	0.000	-
16	β -Thujone	1120	1114	895	57087	896	52588	135.454	148.909	48.767	49.765
17	trans-Pinocarveol	1143	1139	887	4458	-	-	1.841	-	2.263	-
18	Borneol	1174	1165	891	33002	892	30292	42.580	45.591	14.182	14.625
19	4-Terpineol	1183	1177	900	44096	886	37072	57.102	58.992	15.904	16.400
20	α -Terpineol	1198	1189	913	16567	902	15261	15.234	17.996	4.641	4.736
21	Myrtenal	1198	1193	903	13368	874	12271	21.345	18.852	7.579	7.815
22	7-Methyl-3-octen-2-one	1204	-	843	1165	803	1114	1.248	1.279	0.394	0.403
23	cis-Piperitol	1213	1193	859	2035	882	1868	1.134	1.256	0.668	0.689
24	Nerol	1228	1228	807	1355	844	1139	1.826	2.240	0.602	0.619
25	Cuminic aldehyde	1244	1239	861	3089	860	2836	2.294	2.263	1.025	1.057
26	Bornyl acetate	1287	1285	910	8634	918 ^b	8257	6.243	6.450	1.414	1.458
27	Sabinyl acetate	1293	1291	939	4675	864 ^b	4291	1.281	-	1.186	-
28	α -Terpinil acetate	1350	1350	876	29759	879	25019	14.014	15.140	5.269	7.870
29	α -Copaene	1381	1376	896	7647	909	7044	3.616	3.343	1.376	1.419
30	Unknown	1381	-	-	31021	-	28474	15.042	18.534	5.693	5.869
31	Sabinyl isobutyrate	1416	1416	890 ^c	65107	912 ^c	59761	76.197	71.710	21.347	22.014
32	β -caryophyllene	1425	1418	906	42265	908	40419	23.470	23.208	6.945	7.087
33	trans- β -farnesene	1459	1458	871	35327	876	32425	21.491	23.573	6.891	7.106
34	Unknown	1469	-	-	10659	-	9784	5.545	5.772	1.853	1.891
35	Germacrene D	1488	1480	900	21754	881	20804	14.768	14.192	5.276	5.441
36	Biciclogermacrene	1502	1494	869	10547	-	-	7.875	-	1.786	-
37	Sabinyl isovalerianate	1506	1503	906 ^c	71628	905 ^c	60219	76.137	86.920	39.133	40.355
38	β -bisabolene	1515	1509	890	3808	782	3508	1.745	1.389	0.439	0.453
39	Sabinyl valerianate	1519	1516	892 ^c	62671	896 ^c	57524	93.136	95.015	27.224	28.074
40	δ -cadinene	1526	1524	846	9409	858	8998	5.033	4.948	1.698	2.536
41	γ -undecalactone	1579	1606	867	1963	902	1802	1.208	1.296	0.560	0.578
42	Spathulenol	1585	1576	874	46948	805 ^b	39470	57.990	-	15.830	-

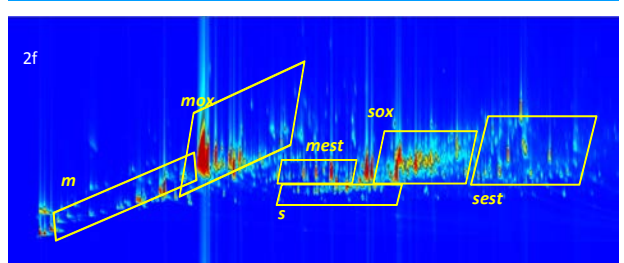
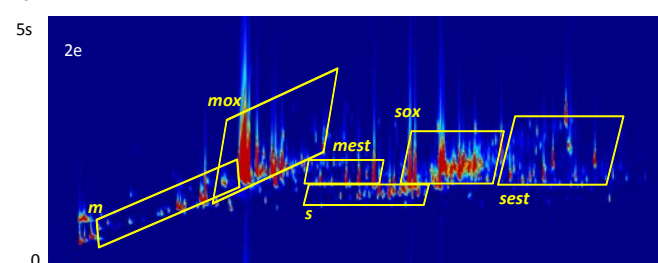
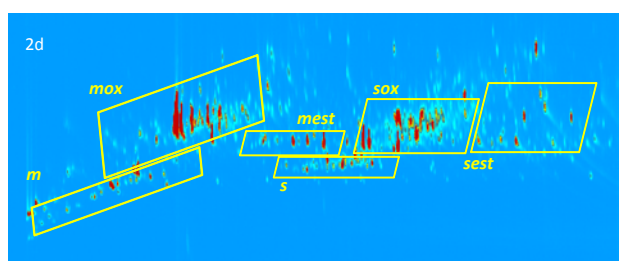
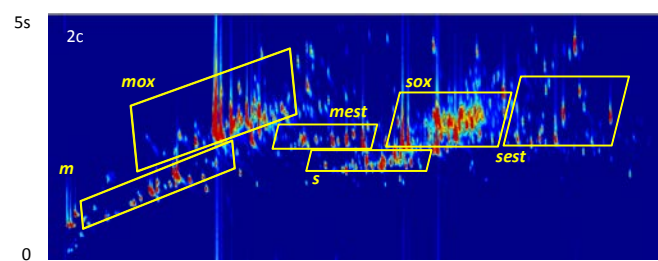
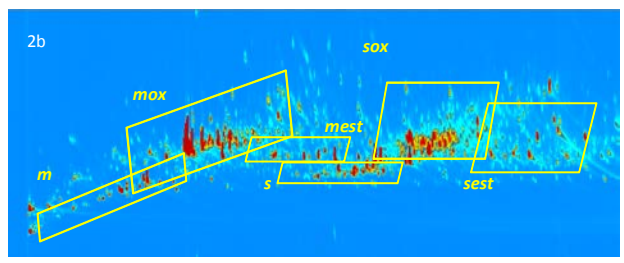
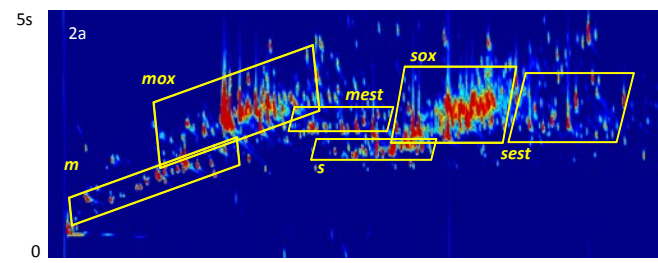
43	Neryl isovalerianate	1587	1584	817 ^c	60494	896 ^c	55527	1.942	112.811	31.251	32.226
44	Caryophyllene oxide	1589	1581	905	28691	890 ^b	27437	31.000	84.891	11.036	28.262
45	Unknown	1632	-	-	36098	-	33133	0.098	0.137	15.677	16.167
46	Unknown	1675	-	-	14160	-	11905	25.263	23.381	4.651	4.785
47	γ -dodecalactone	1686	1671	817	1038	854	956	1.294	1.657	0.429	0.442
48	Unknown	1895	-	-	4419	-	4056	3.395	3.374	1.515	1.562
49	Unknown	1918	-	-	14011	-	12861	13.989	14.268	4.327	4.462
50	Unknown MW 232	1951	-	-	10077	-	9637	11.791	12.280	4.034	4.632
51	Unknown	2056	-	-	12421	-	11401	10.115	10.479	3.026	3.120

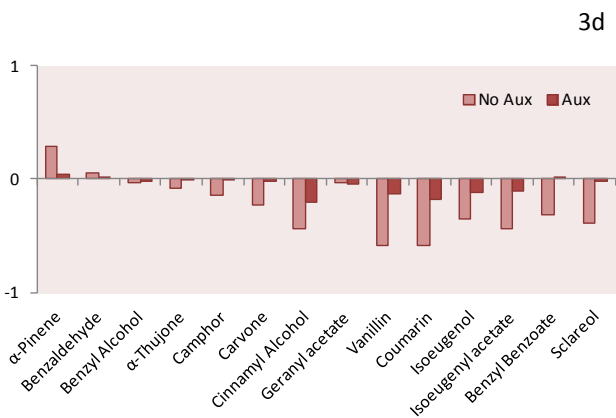
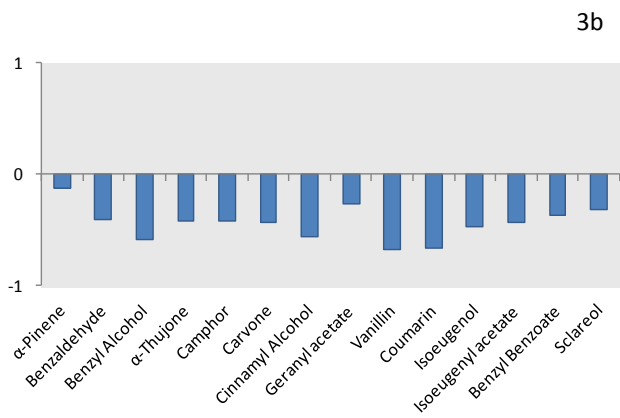
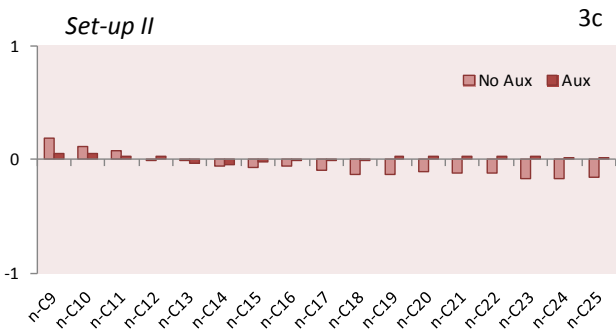
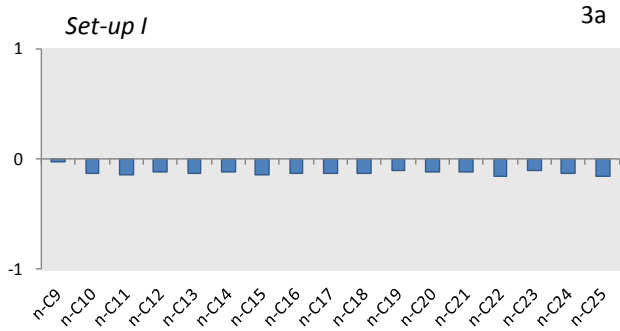
^a: Adams Essential Oils database Ref. 28

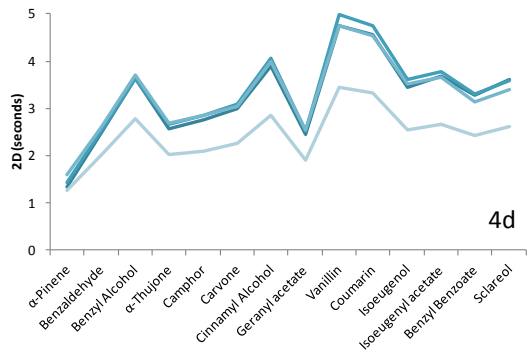
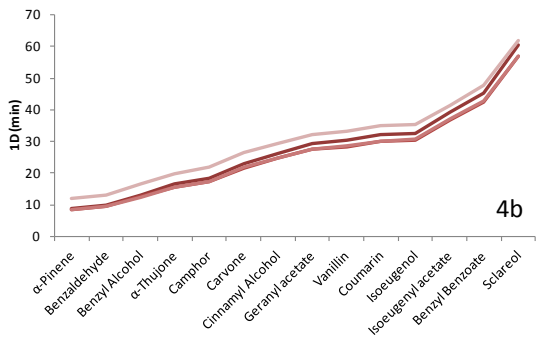
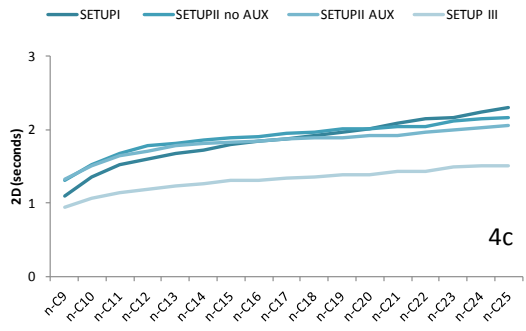
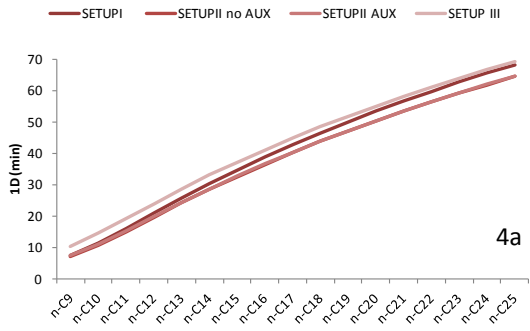
^b: partial coelution

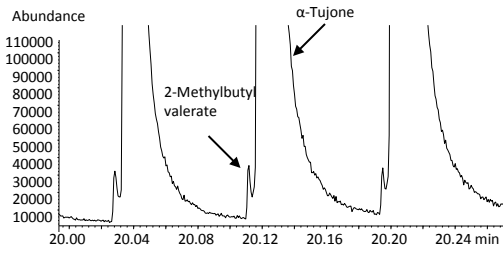
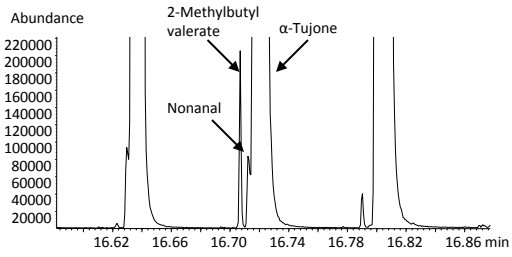
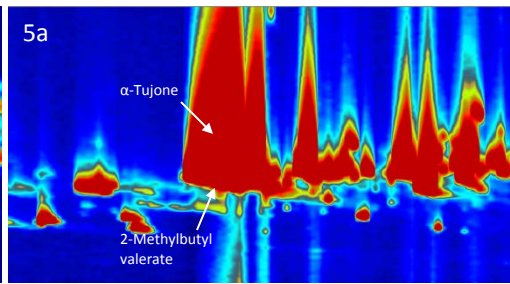
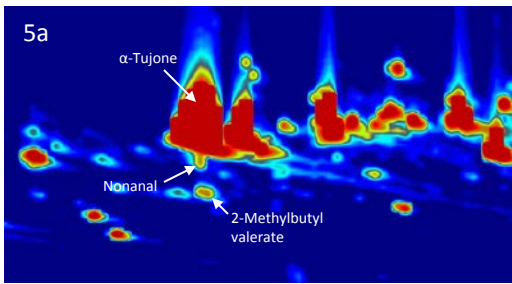
^c: authentic standards ad-hoc synthesized Ref. 25



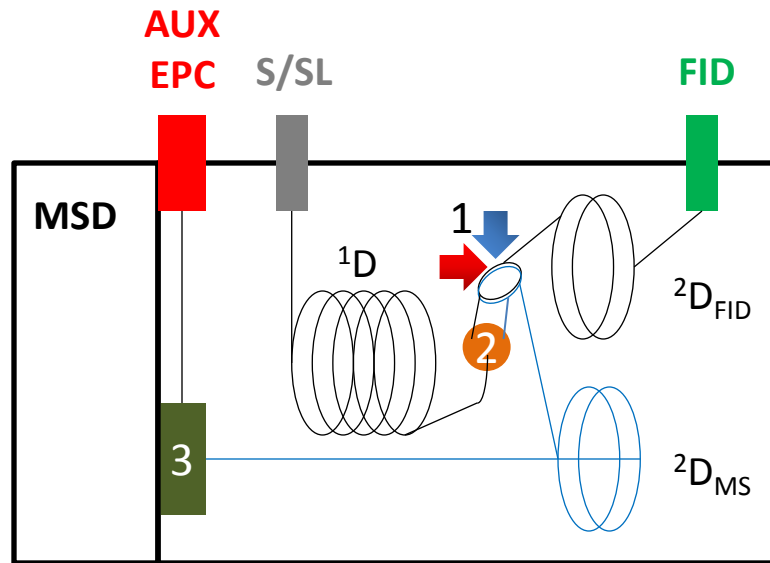








1. Loop-Type thermal modulator
(Zoex Corporation, Houston, TX)



2. Microfluidic 3-port splitter
(Sil-flow™- SGE Ringwood,
Victoria, Australia)

3. Outlet pressure compensation
Microfluidic device (Quick-Swap™- Agilent)